ARMA 21–1238

Support Design Using the Ground Reaction Curve and Support Reaction Curves at Underground Limestone Mines.

Castillo, J., Cardenas Triana, C. and Agioutantis, Z.
Department of Mining Engineering, University of Kentucky, Lexington, Kentucky, U.S.A.

ABSTRACT: Support of underground openings is typically accomplished at the intersection of the ground reaction and support reaction curves which represents an equilibrium point between the driving and resisting forces. This point can be used to select appropriate support systems during entry development. Literature suggests that the pillar structures in underground mines can also be regarded as support structures and their reaction to tributary and additional (abutment) stress can be viewed with respect to the ground reaction curve at the pillar location. This paper presents a series of 2D and 3D finite element numerical models that were used to estimate the ground reaction curve and the support reaction curve for a production pillar at an underground limestone mine. Numerical models take into account the stages of development and benching around the pillar. The equilibrium point between the ground and support reaction curve was estimated for the pillar under investigation. The numerical models show that the pillars react to the overburden load during development and production by deforming in the vertical direction in the order of 7-10 mm.

1. INTRODUCTION

The development of underground excavations induces changes in the in-situ stresses of the rock mass. These changes are not produced by externally applied loads, but are the result of the rock mass restoring the equilibrium that was perturbed by the excavation.

Over time, many hypotheses have been formulated to explain the in-situ state stress of the earth's crust and its causes. Nonetheless, it is very difficult to measure the in-situ stresses without changing them in the process. As a result, such measurements may not be completely valid (Caudle and Clark, 1955).

There are more than 120 operating underground stone mines in the United States that use the room-and-pillar method of mining. The function of pillars in this method is to provide both local and global stability. Local stability is defined as the provision of stable ribs and stable roof conditions that allow safe access to working areas. Global stability is defined as the need to support the weight of the overburden strata up to the ground surface (Esterhuizen et al., 2011.)

Although there are three main design approaches for the analysis of the stability of underground openings, i.e. the numerical approach, the analytical approach, and the empirical approach (Ray et al., 2019), the design of mine structures has been broadly based on experience-based (empirical) methods. This also applies to pillar design methodology, which relies on the calculation or estimation of the stresses acting on the pillar and the stresses the pillar can bear before failing. In general terms, and in order to ensure stability, pillar strength needs to be greater than the stresses imposed to the pillar by the overlying strata. This approach, however, relies on accurate estimates of stresses and pillar strength. The stresses acting on a pillar can be calculated in various ways, such as the tributary area theory, the pressure arch theory as well as the theory of abutment stresses (with applications in coal mining and other areas), which are methods that are mainly based on geometry. Pillar strength has been extensively estimated using empirical approaches. These calculations do not always take into consideration the complex geology, the different stress states, or the effect of the in-situ stresses. In addition, they do not necessarily consider pillar deformations as stresses on the pillar increase.

This paper presents the utilization of numerical modeling to assess the Ground Reaction Curve (GRC) at an underground limestone excavation and the Support Reaction Curve (SRC) as it pertains to pillars in order to investigate their application for assessing mine stability.

The present work introduces the state of the art of the GRC and SRC in numerous coal mining studies and describes the numerical process to estimate the GRC and SRC for an underground limestone operation, where pillars can be typically considered stiffer than coal pillars. Numerical modeling utilizes two- and three-dimensional finite element method to determine the GRC and SRC and to evaluate the convergence and stresses in an underground limestone mine as the interaction between these two curves can give a wider understanding of the

equilibrium between the overburden response and the pillar strength and can also provide information about the convergence and the stiffness of the support system.

2. PILLAR SUPPORT DESIGN USING THE GRC AND SRC CURVES

2.1 Ground Reaction Curve and Support Reaction Curve

The Ground Reaction Curve describes the decreasing internal pressure of the ground when an excavation is completed. It also shows the convergence produced by the excavation. Convergence is defined as the closure between the roof and the floor between an initial and final state or within a time period. Although, this curve can theoretically be obtained with an analytical solution, nonetheless, this approach has certain limitations due to the assumptions needed (circular excavation, isotropic stress field, homogeneous rock mass and, plain stress conditions). This method started in the tunneling industry and, in recent years, has also been applied to pillar design, as shown in Fig. 1 (Brown et al., 1983).

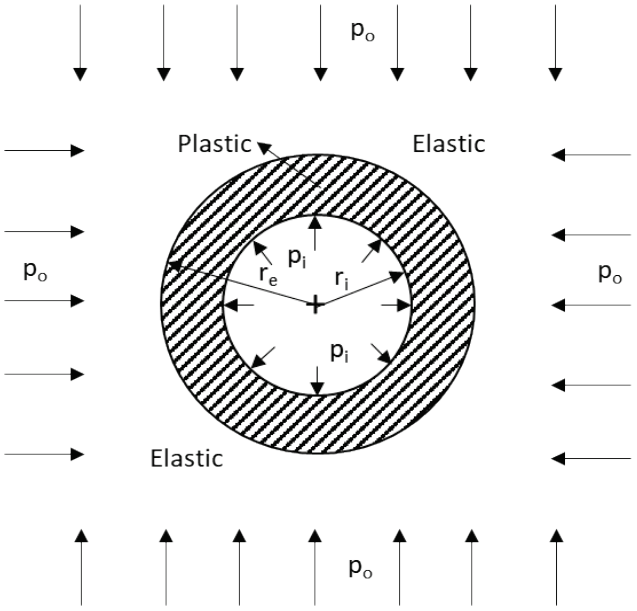

Fig. 1. Axisymettric tunnel problem (Brown et al., 1983)

Fig. 2 shows a conceptual representation of the GRC development. In the A-D curve, point A represents the initial state where the support pressure is equal to the overburden stress, i.e. before any movement occur; this is a theoretical state and it is assumed that there is no convergence. As the underground structure starts absorbing the overburden stress, convergence increases, the excavated ground starts losing its self-supporting capacity, starting from an initial linear response and progressing to a non-linear response (point B). Point C represents the moment in which the required support resistance begins to increase (change in the first derivative). Point D represents the dead weight of the failed ground.

The P-R line represents the response of the support system or the support reaction curve (Esterhuizen et al., 2010a) The SRC, describes the stress-convergence response of a determined support system either man-made (pumpable cribs, concrete cribs and wood cribs) or natural (pillars). For pillars, this curve will describe the amount of stresses the pillar can bear and the corresponding displacements.

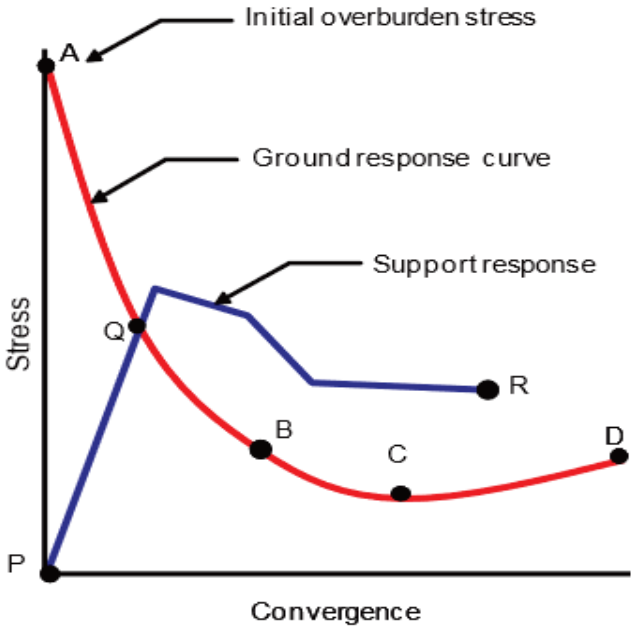

Fig. 2. Conceptual representation of the Ground Reaction Curve and the Support Reaction Curve (Esterhuizen et al., 2010b)

2.2 The GRC for mining applications

The GRC had been estimated for mining purposes multiple times in the past. A few examples with respect to coal mining are given below.

Mucho et al., (1999) estimated the GRC for a longwall mine located in the Pittsburgh coal seam in western Pennsylvania. This mine used a double row of 4-point wood cribs on 4 feet (1.2 m) spacing between supports in adjacent rows for the longwall tailgate stability. The mine also implemented concrete cribs due to the inconsistent timber quality. Since the support's stiffness is different, and the implementation was made in a similar geometrical arrangement. The GRC can be calculated with this information.

Esterhuizen and Barczak, (2006) calculated the GRC for a longwall operation using the FLAC finite-difference model. Then the average convergence in the tailgate entry was recorded.

Barczak et al., (2008) estimated the GRC for a longwall mine by using the FLAC finite-difference model. The

curves were developed by simulating a uniform support pressure on the roof and floor of the tailgate entry while sequentially modeling the four external loading stage.

Esterhuizen et al., (2010a) calculated the GRC by using the FLAC3D finite-difference model for coal mining excavations that used longwall and pillar extraction panels in the United States. Then, the pillar stress and associated convergence were determined.

Damjanac et al., (2014) determined the GRC for the overburden above a longwall coal operation using numerical simulation by gradually reducing the average pressure applied to the roof and determining the corresponding roof displacement in the middle of the panel.

Ray et al., (2019) determined the GRC for the overburden at a longwall coal operation in the eastern US using both a pillar-scale and a panel-scale simulation in FLAC3D. The panel-scale model was used to analyze the strata-pillar interaction. This GRC was obtained by reducing the pillar stiffness simultaneously in all the remaining pillars in the panel.

These studies had established different methodologies to determine the GRC. While most of the research has been conducted in coal mining, these estimation methods can be used in cases of room and pillar layouts in limestone mines.

2.3 The SRC for mining applications

Support systems are employed to support the roof, prevent roof falls and ensure the stability of the mine structure. The SRC represents a support system's capacity as a function of roof convergence. As the stiffness of the support system increases, the allowable convergence decreases.

Barczak (2003) determined the SRC for pumpable cribs by performing laboratory tests and using underground coal mine instrumentation. He also stated that human-made supports are incapable of providing sufficient load capacity to eliminate all convergence. The convergence that cannot be controlled by the installed support system, was termed uncontrolled convergence.

A significant portion of this uncontrollable convergence is caused by the elastic deformations of the rock mass. As such, the amount of uncontrollable convergence will increase with increasing depth of cover and decreasing pillar size (Barczak et al., 2005) as shown in Fig. 3.

The SRC concept can conceptually be applied for natural support systems such as pillars and, as a result, corresponding curves can be determined. These curves would represent the pillar strength which can be defined as the maximum axial compressive stress a pillar can bear before it fails.

Bieniaswki (1984) postulated that the strength of mine pillars mainly depends on the following factors: (1) the size or volume effect (strength reduction from a small laboratory specimen of rock to full-size mine pillars), (2) the effect of pillar geometry (shape effect), and (3) the properties of the pillar material.

However, in contrast with SRCs for entry supports, which can either be determined in the lab or with insitu measurements, SRCs for pillars can only be determined using numerical modeling.

The following sections present information related to numerically modeling pillar behavior for different pillar geometries and extraction ratios, in order to determine the corresponding SRCs.

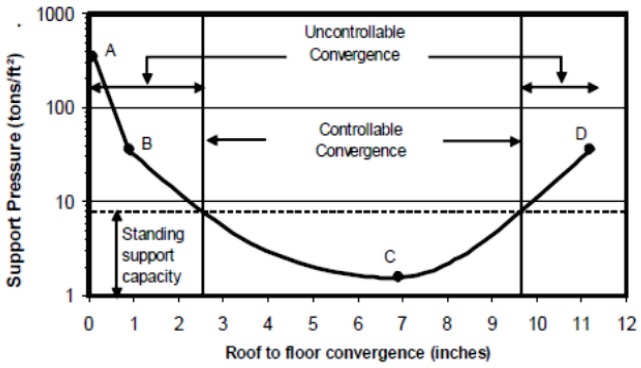

Fig. 3. Uncontrollable and controllable convergence (Barczak et al., 2005)

2.4 The GRC and SRC equilibrium point

The GRC and SRC generated through finite element numerical models are superposed and the intersection is considered the equilibrium point. This point reflects the value of the convergence, the stress state and the stiffness of the support system.

Damjanac et al., (2014) calculated the SRC for different extraction ratios varying from 50% to 90%, then they superimposed this with the expected GRC for their case. The authors demonstrate that as the extraction ratio increased the average pillar strength decreased. The SRC and GRC intersected at a higher equilibrium point when the lower extraction ratio was modeled. For a 50% extraction ratio, the roof displacement was approximately 0.07 m, and the average pillar strength was 11 MPa.

Esterhuizen et al., (2010b) calculated the SRC for pillars with different width-to-height ratios and the GRC for different span values. The SRC calculated in this study shows that a higher width-to-height ratio will yield a higher pillar strength. However, if the width-to-height ratio is higher than 8 an evident peak strength is not identifiable because pillars deformation is governed by strain hardening. The GRC for different span values shows that for greater spans the stress transferred to the

abutment pillars by arching decreases. For a width-to-height of 8 and a span of 1000 ft (300 m) the pillar and the rock mass will come to equilibrium at a stress of 10.8 MPa stress and 0.7% strain.

3. NUMERICAL MODELING

This section presents a series of finite element numerical models that were used to estimate the ground reaction curve and the support reaction curve for a pillar in an underground limestone mine. Numerical models take into account the stages of development and benching around the pillar.

Modeling of the pillar response to loading and failure was used to determine the SRC, while modeling the pillar response with respect to a decreasing pillar stiffness was used to determine the GRC. All models were developed using the RS2 and RS3 finite element packages by RocScience. Table 1 summarizes the four different models developed for this investigation; models were developed using stages so that loading conditions could be applied in a stepwise manner.

Table 1: Finite Element Models for SRC and GRC

Model	2D	3D
SRC	SRC-2D	SRC-3D
GRC	GRC-2D	GRC-3D

3.1 Mohr-Coulomb failure criterion

The Mohr-Coulomb failure criterion has been widely used for rock mechanics applications. This criterion involves Coulomb's hypothesis, which predicates a linear relationship between the shear strength on a plane and the normal stress that acts on it. The general form of the equation is as follows:

$$\sigma_1 \geq c\frac{2cos\varphi}{1-sin\varphi} + \sigma_3\frac{1+sin\varphi}{1-sin\varphi}$$

where σ_1 and σ_3 are the major and minor principal stresses, c is the cohesion, and φ is the angle of internal friction of the rock.

For some cases, peak and residual values for the cohesion and friction angle can be entered. Thus, after the initial yielding, the material's strength will drop from the peak state to a lower state.

3.2 Hoek-Brown failure criterion

The Hoek-Brown criterion is a non-linear relationship and was introduced for the design of underground excavations in hard rock (Hoek et al., 2002). It was derived from the research into the brittle failure of intact rock by Hoek (1968) and on model studies of jointed rock-mass behavior by Brown (1970).

The equation that describes the model is as follows:

$$\sigma_1 \geq \sigma_3 + \sigma_{ci}\left(m_b + \frac{\sigma_3}{\sigma_{ci}} + s\right)^a$$

where σ_1 and σ_3 are the major and minor principal stresses, σ_{ci} is the unconfined compressive strength of the rock, and m_b, s and a are empirically derived material constants.

3.3 Model Properties

The material properties used for modeling limestone were retrieved from the literature and are presented in Table 2. The Mohr-Coulomb criterion was transformed to the Hoek-Brown criterion using the RocData software program (by Rocscience). This is accomplished by determining a linear envelope that provides the "best fit" between the two failure criteria over a given stress range. The failure envelope range for this study was set to "General" in RocData. This assumes that the maximum σ_3 is one fourth of the uniaxial compressive strength of the intact rock.

It should be noted that this study utilizes the Mohr-Coulomb and Hoek-Brown criteria to model pillar response and not empirical pillar strength criteria that were used by other studies indicated above.

Table 2: Mohr-Coulomb parameters for modeling limestone material used by Esterhuizen et al., (2010a)

UCS (lab value)	100 MPa
Young's modulus (lab value)	40 GPa
Poisson's ratio	0.3
Peak Cohesion	15.1 MPa
Peak Friction Angle	40 deg
Peak Tensile Strength	5 MPa
Dilation Angle	10 deg

3.4 Determination of the SRC in 2D

The SRC was determined from the average stress-strain curve at the top of the pillar.

Fig. 4 shows the part of the mine geometry, which utilizes a room and pillar layout. The modeled pillar is 93 ft (28.3 m) long by 34 ft (10.4 m) wide on 150 ft (45.7 m) by 90 ft (27.4 m) centers. The SRC-2D model was generated using section A-A' as shown in Fig. 4. The width of the SRC model is 90 ft (27.4 m).

Fig. 5 shows the cross-section of the SRC-2D model which was developed using 11 stages. Stage 1 corresponds to insitu conditions before excavation commences; stage 2 corresponds to the development phase (excavation of entries and cross-cuts) where the pillar has a width-to-height ratio of 1.19; stage 3 corresponds to the fully extracted entries, and cross-cuts (benched entries) and full exposure of the pillar to vertical and horizontal stresses (the benched width-to-height ratio is 0.56); and stages 4-11 correspond to a displacement control loading applied at the top boundary of the model.

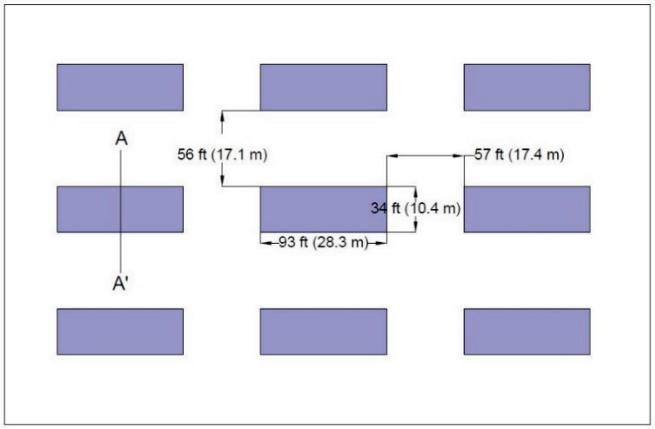

Fig. 4. Plan view of room and pillar layout and 2D section information

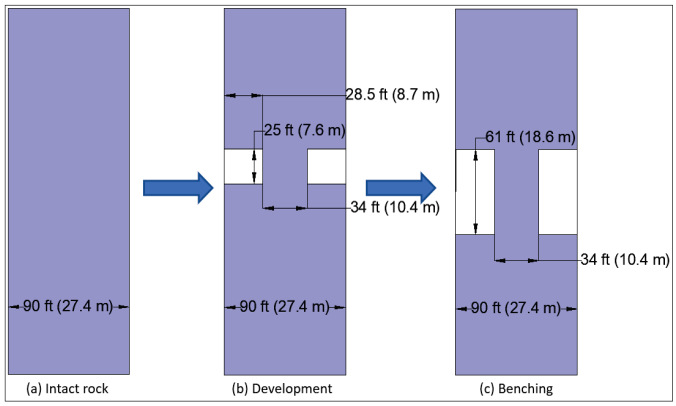

Fig. 5. Cross-section of the SRC-2D model with stages.

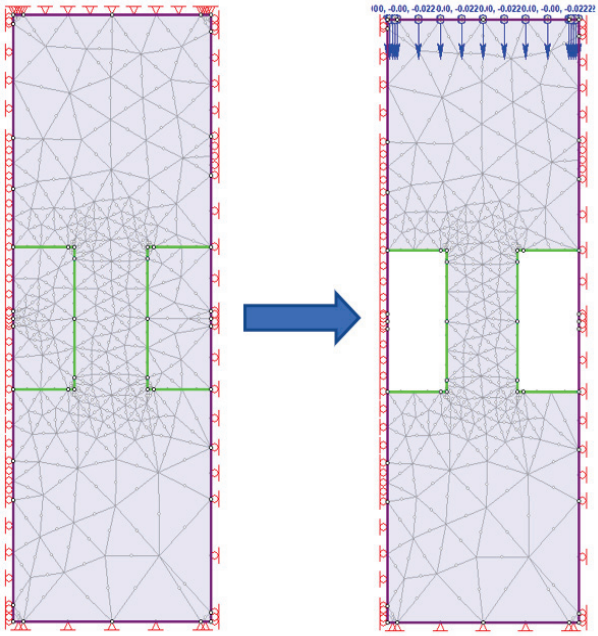

Fig. 6. SRC-2D model with mesh, excavations, and boundary conditions

Fig. 6 shows the model with the boundary conditions. The lateral model boundaries were constrained in the X direction (this is represented by a red circle at the sides of the model), the bottom and top boundary was constrained in the X and Y directions (this is represented by a red triangle at the bottom and top of the model). After the excavation was introduced, a vertical displacement was applied to the top boundary of the model through the different stages (this is represented by the blue arrows pointing in a downwards direction).

3.5 Determination of the SRC in 3D

Fig. 7 shows the boundary conditions of the SRC-3D model, in which the lateral boundaries were constrained in the X and Y directions. The SRC-3D model was also developed using 11 stages as stated before. The bottom boundary was constrained in all three directions, and a downward displacement was applied on the top boundary. Thus, the movement was only allowed in a vertical direction. After the excavation was introduced, a vertical displacement was applied to the top boundary of the model through stages 4 – 11 (this is represented by the arrows pointing in a downwards direction).

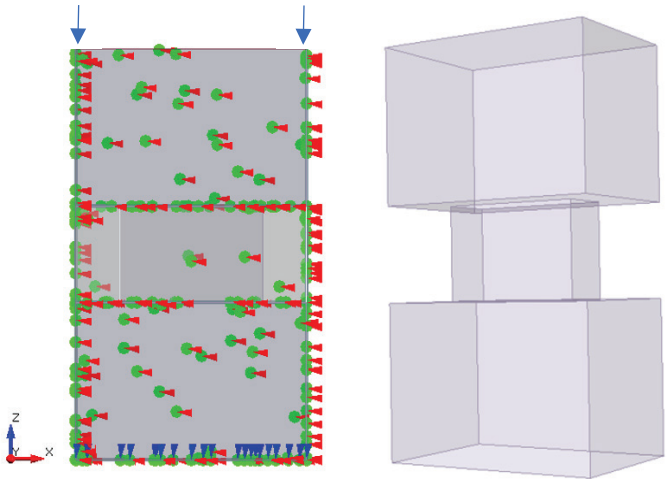

Fig. 7. SRC-3D model with boundary conditions.

3.6 Determination of the GRC in 2D

The GRC-2D model was generated using section B-B' in Fig. 8. The width of the model is 270 ft. (82.2 m).

Fig. 9 shows the GRC-2D model with the boundary conditions imposed, where the left and right boundaries of the model were constrained in the X direction, the lower boundary was constrained in the X and Y directions, and the top boundary was free. The model was developed using 13 stages. Stage 1 corresponds to gravitational load of the overburden (insitu stress); stage 2 corresponds to entry and cross-cut development; stage 3 corresponds to the fully extracted entries (i.e., after benching) and full exposure of the pillar. To obtain the pillar's response (GRC) to different loading conditions, the pillar's stiffness was changed between different model runs, in a stepwise manner, i.e., from 100% to 0.0001% of the stiffness. This corresponds to the stages 4 – 13.

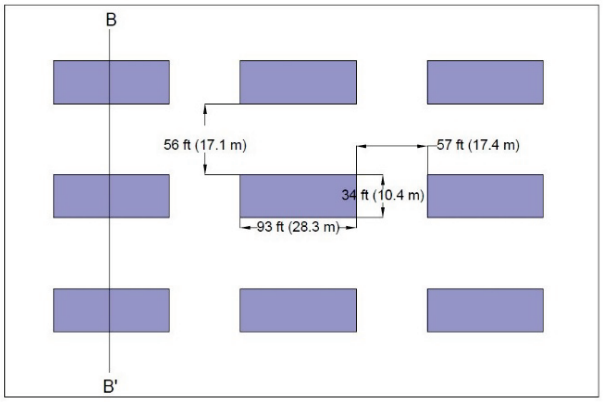

Fig. 8. Plan view of room and pillar layout and 2D section information.

3.7 Determination of the GRC in 3D

The GRC-3D model was run in stages in the same manner as the GRC-2D model. Once the initial loads are applied to model, then the excavated openings are introduced. The boundary conditions for the bottom of the model were to restrain the displacements in the X, Y, and Z directions (Fig. 10). The lateral boundary conditions included restraints in both the X and Y direction, and thus, the movement was only allowed along the vertical axis. Boundary conditions were not applied at the top of the model as that represents the free surface. Loading of the model was performed using the "gravity load" option of the software program. To obtain the response (GRC) of the center pillar to different loading conditions, its stiffness was changed between different model runs from 100% to 0.0001%.

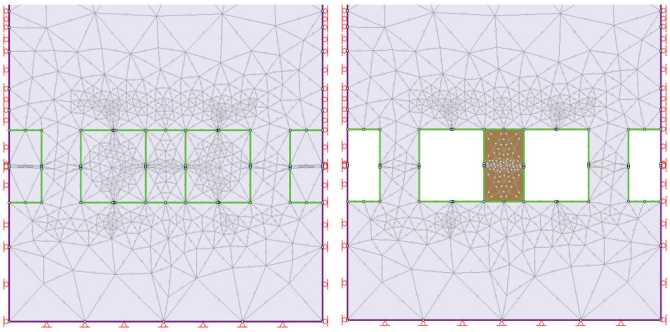

Fig. 9. GRC-2D Model with mesh, boundary conditions, and excavated openings.

4. RESULTS AND DISCUSSION

Fig. 11 compares the pillar behavior (which corresponds to the SRC) under the Mohr-Coulomb and the Hoek-Brown criteria using both 2D and 3D models. The SRC elastic responses for both 2D and 3D models are the same. The pillar deformation at the peak stress of 50 MPa (7252 psi) is 41 mm (1.61 inches). The response in the post-peak regime is similar between the two models, however the Hoek-Brown criterion reaches a lower residual strength.

The GRC for the 2D case is also plotted in Fig. 11. The behavior of this curve is as expected, i.e., the convergence starts at zero and gradually increases, while the stress decreases. The GRC starts with a stress value of 21 MPa (3046 psi) and descents to 0 MPa (0 psi).

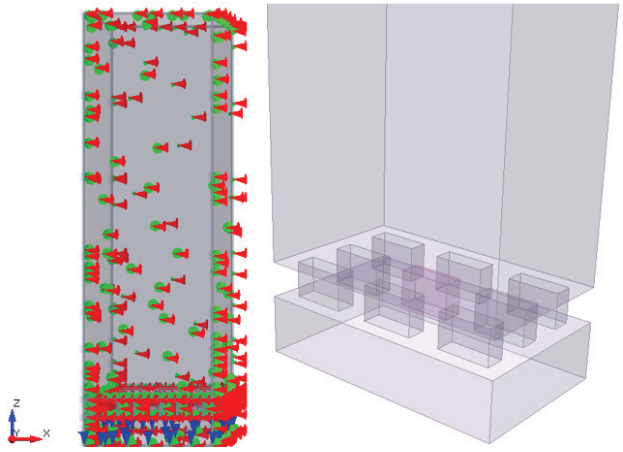

Fig. 10. GRC-3D model with boundary conditions and excavated openings.

It should be noted that although the maximum deformation of the pillar is the same for both criteria, the behavior in the post peak zone is different.

For the 3D case, it can be observed that the pillar deformation for the Mohr-Coulomb criterion, as well as the Hoek-Brown criterion at 29.1 MPa (4220 psi), is 24.2 mm (0.95 inches). Although the two models behave in a similar manner the Hoek-Brown criterion results in slightly higher post-peak stresses.

The GRC that was developed by 3D modeling is also plotted in Fig. 11. The GRC starts with a pressure value of 17 MPa (2465 psi) and descends linearly to 0 MPa.

The point at which the GRC and the SRC intersect is the equilibrium point. The equilibrium point for the 2D model is located at a stress value of 12 MPa (1740 psi) with a pillar deformation of 10 mm (0.39 inches). The equilibrium point for the 3D model is located at a stress value of 8 MPa (1160 psi) with a pillar deformation of 7 mm (0.27 inches).

Fig. 11 helps visualize the SRCs and GRCs for the 2D and 3D models. The SRCs for the 2D model reach higher stress values as the 2D models imply a pillar with infinite length. Similarly, the GRCs for the 2D models provide for higher stress and deformation as the 2D models correspond to structures with an infinite third dimension. Esterhuizen et al., (2011) concluded that underground mines should avoid slender pillars because the confining stresses within the pillar approaches zero, and, therefore, the likelihood for these pillars to fail is higher. However, the approach used in that study was based on the tributary area theory coupled with empirical equations for pillar

strength and it did not consider pillar deformation during loading.

The approach in this study combines both the response of the overburden and pillar deformation as given by two commonly utilized failure criteria without using empirical strength equations. A combination of these two approaches could result in optimal pillar design practices for underground limestone mines.

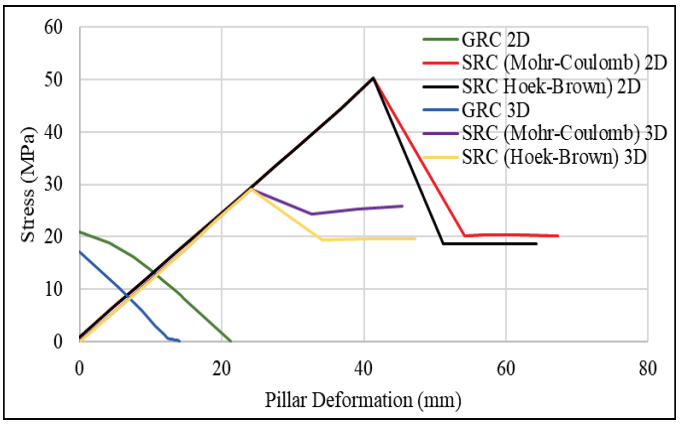

Fig. 11. Results of 2D and 3D models

The Ground Reaction Curve allows for overburden deformation to be included in the stress balance before and after an excavation. Thus, the overburden response mechanism can be represented not just by action and reaction forces, but by including both the deformation of the roof and the pillar. Numerical modeling is primarily used to determine this curve, although empirical solutions or measurements can be used to verify results by providing specific points on the curve.

5. CONCLUSIONS

The Support Reaction Curve generated by the two-dimensional models is similar to the one generated by the three-dimensional models. The first part of the SRC is linear and corresponds to the elastic response of the rock mass before the failure criteria are engaged. The difference between the two curves can be explained by the fact that a plane strain 2D model refers to an infinitely long pillar while a 3D model accounts for the finite dimensions of each pillar. Hence the SRC for a 2D model can reach higher stress values than the SRC for a 3D model.

Numerical results indicate that the Support Reaction Curve extends above the Ground Reaction Curve. This indicates that the pillar can likely take a higher load than the load applied during the benching process. Pillars are expected to deform in the vertical direction by 7-10 mm (3D and 2D results respectively).

6. ACKNOWLEDGEMENTS

This study was sponsored by the Alpha Foundation for the Improvement of Mine Safety and Health, Inc. (*ALPHA FOUNDATION*). The views, opinions and recommendations expressed herein are solely those of the authors and do not imply any endorsement by the *ALPHA FOUNDATION*, its Directors and staff.

The authors would also like to acknowledge the help of Dr. Chris Newman of Appalachian Mining & Engineering Inc.

REFERENCES

1. Barczak, T. 2003. Longwall tailgates: the technology for roof support has improved but optimization is still not there. In *Proceedings of the Longwall USA, International Exhibition and Conference*. Pittsburgh, PA. 105-130.

2. Barczak, T.M., G.S. Esterhuizen, and D.R. Dolinar. 2005. Evaluation of the impact of standing support on ground behavior in longwall tailgates. In *Proceedings of the 24th International Conference on Ground Control in Mining*. Morgantown, WV. 23-32.

3. Barczak, T.M., G.S. Esterhuizen, G.L Ellenberger, and P. Zhang. 2008. A first step in developing standing roof support design criteria based on ground reaction data for Pittsburgh seam longwall tailgate support. In *Proceedings of the 27th International conference on ground Control in Mining*. Morgantown, WV. 349-359.

4. Bieniawski, Z.T. 1984. *Rock mechanics design in mining and tunneling*. No.5 Monograph.

5. Brown, E.T. 1970. Strength of models of rock with intermittent joints. *J. Soil Mech. Found. Div,* Vol 96. No 6. 1935-1949.

6. Brown, E.T., J.W. Bray, B. Ladanyi, and E. Hoek. 1983. Ground response curves for rock tunnels. *Journal of Geotechnical Engineering.* 109(1), 15-39.

7. Caudle, R.D., and G.B. Clark. 1955. *Stresses around mine openings in some simple geologic structures*. University of Illinois Bulletin. Vol. 52, Number 69.

8. Damjanac, B., M. Pierce, and M Board. 2014. Methodology for stability analysis of large room-and-pillar panels. In *Proceedings of the 48th US Rock Mechanics/Geomechanics Symposium. Minneapolis, MN*: American Rock Mechanics Association, paper 14-7199.

9. Esterhuizen, G.S., and T.M. Barczak. 2006. Development of Ground Response Curves for Longwall Tailgate Support Design. In *Proceedings of the 41st U.S. Rock Mechanics Symposium*. Golden, Colorado. 17-21.

10. Esterhuizen, G.S., C. Mark, and M.M. Murphy. 2010a. Numerical model calibration for simulating coal pillars, gob and overburden response. In *Proceedings of the 29th International Conference on Ground Control in Mining*. Morgantown, WV. 46-57.

11. Esterhuizen, G.S, C. Mark, and M.M. Murphy 2010b. The ground response curve, pillar loading and pillar failure in coal mines. In *Proceedings of the 29th International Conference on Ground Control in Mining.* Morgantown, WV. 19-27.

12. Esterhuizen, G.S., D. Dolinar, and J. Ellenberger. 2011. Pillar strength in underground stone mines in the United States. *International Journal of Rock Mechanics and Mining Sciences.* 48(1) 42-50.

13. Hoek, E., 1968. Brittle fracture of rock. Chapter 4, Rock mechanics in engineering practice, 99-124. Wiley.

14. Hoek, E., C. Carranza-Torres, and B. Corkum. 2002. Hoek-Brown failure criterion-2002 edition. In Proceedings of the NARMS-Tac. 267-273.

15. Mucho, T.P., T.M. Barczak, D.R. Dolinar, J. Bower, and J.J. Bryja. 1999. Design Methodology for Standing Secondary Roof Support in Longwall Tailgates. In *Proceedings of the 18th International Conference on Ground Control in Mining*. Morgantown, WV. 136-148.

16. Ray, R., Z. Agioutantis, and K. Kaklis. 2019. Mine Pillar Design Using the Ground Reaction Curve Concept. In *Proceedings of the 38th International Conference on Ground Control in Mining*. Morgantown, WV. Society for Mining, Metallurgy & Exploration. 204-211.